Asymmetrical Precipitation Sensitivity to Temperature Across Global Dry and Wet Regions

Juan Liang, Xianfeng Liu, Amir Aghakouchak, Philippe Ciais, Bojie Fu

Earth's Future

RESEARCH ARTICLE
10.1029/2023EF003617

Special Section:
CMIP6: Trends, Interactions, Evaluation, and Impacts

Asymmetrical Precipitation Sensitivity to Temperature Across Global Dry and Wet Regions

Juan Liang[1], Xianfeng Liu[1,2], Amir AghaKouchak[3], Philippe Ciais[2], and Bojie Fu[1,4]

[1]School of Geography and Tourist, Shaanxi Normal University, Xi'an, China, [2]Laboratoire des Sciences du Climat et de l'Environnement, CEA-CNRS-UVSQ, Gif-sur-Yvette, France, [3]Department of Civil and Environmental Engineering, University of California, Irvine, CA, USA, [4]State Key Laboratory of Urban and Regional Ecology, Research Center for Eco-Environmental Sciences, Chinese Academy of Sciences, Beijing, China

Abstract Global warming is expected to increase precipitation extremes. However, the response of extreme precipitation to global warming in various climates remains unclear. Here, we analyzed changes in the sensitivities of extreme and mean precipitation to temperature across the dry and wet regions of the world during 1960–1999 and 2060–2099 using global climate models. Both extreme and mean precipitation exhibited similar spatial patterns; however, the magnitude of sensitivity for extreme precipitation was approximately three times higher (19%/K) than for mean precipitation (6%/K). A higher precipitation sensitivity to temperature was observed in the dry regions than in the wet regions. Dry regions exhibited a four- to five-fold higher temperature sensitivity for mean precipitation, and marginally higher temperature sensitivity for extreme precipitation than wet regions. These findings highlight the importance of implementing adaptive strategies to alleviate the effects of global warming on dryland ecosystems.

Plain Language Summary Global warming alters the precipitation regimes and poses significant risks to ecosystems and humans. In this study, we investigated how mean and extreme precipitation responds to projected warming across global dry and wet regions. We found that the sensitivity of extreme precipitation was three times greater than that of global mean precipitation over land (which implies that global warming is expected to alter extreme precipitation more than mean precipitation). Our results also suggest greater sensitivity in dry regions than in wet regions, indicating that warming is expected to cause higher rainfall variability in dry regions than in wet regions.

Key Points:

- The sensitivity of precipitation to temperature is latitude dependent, increasing over high latitudes and decreasing in mid-latitude regions
- The response of extreme precipitation to global warming is approximately three times larger (19%/K) than that for mean precipitation (6%/K)
- Both extreme precipitation and mean precipitation show a greater sensitivity to temperature across global dry regions relative to wet regions

Supporting Information:

Supporting Information may be found in the online version of this article.

Correspondence to:

X. Liu,
xianfeng.liu@lsce.ipsl.fr

Citation:

Liang, J., Liu, X., AghaKouchak, A., Ciais, P., & Fu, B. (2023). Asymmetrical precipitation sensitivity to temperature across global dry and wet regions. *Earth's Future*, *11*, e2023EF003617. https://doi.org/10.1029/2023EF003617

Received 24 FEB 2023
Accepted 2 AUG 2023

Author Contributions:

Conceptualization: Xianfeng Liu
Data curation: Juan Liang
Formal analysis: Juan Liang, Xianfeng Liu, Amir AghaKouchak, Philippe Ciais, Bojie Fu
Investigation: Juan Liang, Xianfeng Liu
Methodology: Juan Liang, Xianfeng Liu

1. Introduction

Global warming is expected to amplify the hydrologic cycle, causing a large increase in atmospheric water vapor content (O'Gorman & Schneider, 2009), which balances radiative and sensible heat changes with rising temperatures (Held & Soden, 2006; Pendergrass & Hartmann, 2014). Extreme precipitation is likely to intensify with warming at a rate consistent with the water-holding capacity of the atmosphere, ∼7%/K, according to the Clausius−Clapeyron (C−C) equation (Berg et al., 2013; Lehmann et al., 2015; Prein et al., 2017; Trenberth, 2011), In contrast, short-duration (in particular at hourly) precipitation response to warming at double the C−C rate has been observed across diverse regions worldwide (IPCC AR6; Seneviratne et al., 2021). However, global-mean precipitation averages (totals) are constrained, and are expected to increase at a lower rate of ∼1%–3% per degree of warming (Allen & Ingram, 2002, see Section 8.2, IPCC AR6; Douville et al., 2021). Recently, there have been significant trends in temperature and precipitation extremes across many regions worldwide (Fischer & Knutti, 2015; Wei et al., 2019; Zhang et al., 2020), causing devastating effects on human and natural systems (AghaKouchak et al., 2020; Barbero et al., 2017; Easterling et al., 2000; Liu et al., 2009; Min et al., 2011). Examining changes in the precipitation response to temperature is critical for understanding the impact of climate change on future climate risk (Min et al., 2011).

Accumulating evidence has shown that the increase in extreme precipitation worldwide is associated with an increased temperature (Allen & Ingram, 2002; Barbero et al., 2017; Frei et al., 2006; Screen & Simmonds, 2014; Trenberth et al., 2003) and that extreme rainfall occurs differently than changes in mean precipitation. Using CMIP5 climate models, a previous study found that the increase in extreme and mean precipitation across climate scenarios is similar in the tropics but that the increase in extremes is smaller relative to the mean at high latitudes. In contrast to mean precipitation, changes in extreme precipitation did not depend on the emission scenarios

Resources: Juan Liang, Xianfeng Liu
Validation: Xianfeng Liu, Amir AghaKouchak, Philippe Ciais, Bojie Fu
Writing – original draft: Juan Liang, Xianfeng Liu
Writing – review & editing: Xianfeng Liu, Amir AghaKouchak, Philippe Ciais, Bojie Fu

(Pendergrass et al., 2015). John et al. (2022) assessed the changes in precipitation extremes and their uncertainties using a global ensemble of climate models from CMIP6 and demonstrated a robust enhancement of extreme precipitation in more than 90% of the models, consistent with the C−C rate. Future seasonal changes in extreme and mean precipitation were also investigated in specific regions of interest. It was found that regions with an increase in mean precipitation experienced more extremes in all seasons, whereas those with a decrease in mean precipitation had fewer extremes (Bador & Alexander, 2022). These results highlighted the importance of understanding the differences in the responses of extreme and mean precipitation to temperature.

The response of precipitation to temperature varies regionally. Changing patterns of precipitation might exacerbate the contrast between dry and wet areas (Sun et al., 2020), leading to drier conditions in the dry and wetter conditions in the wet regions when considering the difference between precipitation and evaporation (P−E) (Allan et al., 2010; Greve et al., 2014; Liu & Allan, 2013). A recent study also documented that the projected mean and extreme precipitation changes are positively related in dry regions, whereas no relationship exists in wet regions (Donat et al., 2016, 2019). Global dry and wet regions, including grid cells that are based on their dry or wet status, regardless of their geographical location, are considered to have an adequate degree of spatial aggregation to obtain robust regional results rather than aggregation over a geographical region, which may cause uncertainties due to the large internal variability. Knowledge regarding changes in the sensitivity of projected extreme and mean precipitation to temperature between global dry and wet regions requires further research, as they are essential to understand the effects of global warming.

In this study, we analyzed the spatiotemporal variations in global precipitation and its percentile distribution based on the latest climate models from the Coupled Model Intercomparison Project Phase 6 (CMIP6). We then calculated the changes in the sensitivities of extreme and mean precipitation to temperature in the future (2060–2099) compared with the historical period (1960–1999) over global land areas. Finally, we analyzed the different responses of precipitation to temperature across dry and wet regions. Based on these results, we attempted to address the following two questions: (a) What are the differences in the responses of extreme and mean precipitation to temperature? (b) What is the projected precipitation response to temperature between global dry and wet regions over land?

2. Data and Method

2.1. Data

Considering that CMIP6 models simulate climate extremes more effectively than CMIP5 models, owing to their finer resolution and parameterization improvements (Bourdeau-Goulet & Hassanzadeh, 2021; Chen et al., 2020; Eyring et al., 2016; Grose et al., 2020; O'Neill et al., 2016), we retrieved daily precipitation data from 17 CMIP6 models for the historical simulations (1960–1999) and future simulations until the end of the century (2060–2099) (https://esgfnode.llnl.gov/search/cmip6) (Eyring et al., 2016). Detailed information on the model is presented in Table S1 in Supporting Information S1. We selected 17 models because they are commonly used to study extreme precipitation (Thackeray et al., 2022; Yazdandoost et al., 2021). Only one simulation variant was used for each forcing experiment to ensure equal weighting for each selected model. It should be noted that some studies consider SSP5-8.5 to be an overestimation of the anticipated future warming according to Hausfather and Peters (2020); both moderate and high shared socioeconomic pathways were used (SSP3-7.0 and SSP5-8.5, respectively) to ensure the robustness of the results.

The anomaly of future precipitation change was defined as the difference between two intervals: the baseline (1960–1999) and the projection period (2060–2099). The 99th percentile of the historical period (all days) was used as the threshold for defining extreme precipitation. The difference in the total precipitation volumes for extremes between the two periods was then calculated. Given the different resolutions of various models, the local precipitation sensitivity was performed on a native grid, and a global-mean (area-weighted) result was generated for each model. Finally, the multi-model ensemble mean (MMEM) sensitivity was obtained, and MMEM local metrics were calculated following bilinear remapping to a common $1° \times 1°$ grid to reduce the spread of models and plotting purposes.

2.2. Method

2.2.1. Sensitivity of Precipitation to Temperature

The sensitivity of precipitation to temperature (η, η_{99}) is expressed as the ratio of normalized anomaly precipitation (dP, unit: %) to the global-mean air temperature change (ΔGSAT, unit: K), where η denotes the sensitivity of

mean precipitation to temperature and η_{99} denotes the sensitivity of extreme precipitation to temperature. For η_{99}, the anomaly is the difference in the total amount of extreme precipitation that meets and exceeds the historical 99th percentile threshold between 2060–2099 and 1960–1999. We first calculated the global threshold maps of the 99th percentile of daily precipitation over the historical period (1960–1999) for each model. Subsequently, historical and future precipitation were compared to the threshold to identify the local extreme events. The precipitation volumes of all extreme events and a difference between historical and future were then calculated. The difference was then normalized using the historical precipitation volumes before being divided by ΔGSAT. Notably, all available days were used, rather than just wet days, when calculating the 99th percentile threshold. Therefore, the threshold may be a bit lower for some dry regions, especially those susceptible to the influence of atmospheric circulation patterns, which, in turn, leading to a bit larger η_{99}.

2.2.2. Definitions of Global Dry and Wet Regions

To unravel differences in the sensitivity of precipitation to temperature between global dry and wet regions, we first identified the dry (and wet) grid cells from each model and each year using a percentile-based threshold of 30% (or 70%) of the historical precipitation during 1950–2014 for all global land grid cells. Global dry (or wet) regions are those where the precipitation is lower (or higher) than the threshold. The results from all models and years were then merged to generate the spatial distribution of these regions. The details of the method can be found in a study by Donat et al. (2016). For extreme and mean precipitation, we defined the global dry and wet regions separately using the above method.

2.2.3. Correlation Analysis

Pearson's r was used to calculate the correlation coefficient between the temperature sensitivities of extreme precipitation (η_{99}) and mean precipitation (η). Additionally, a null hypothesis test was performed, in which the distributions underlying the samples were uncorrelated and normally distributed. We selected a two-sided p-value to test non-correlation. For a given sample with a correlation coefficient r, the p-value is the probability that the correlation coefficient r' of random samples A and B with zero correlation would be greater than or equal to $|r|$. Pearson's correlation and p-value tests were performed using the SciPy library within the Python platform, following established statistical guidelines for the preferred significance level and sample size.

3. Results

3.1. Divergent Changes in Projected Precipitation

The multi-model ensemble mean (MMEM) extreme precipitation volumes showed an increase of 73% on land (the future 2060–2099 period minus the historical 1960–1999 period), whereas mean precipitation volumes increased by 24% (Figures 1a and 1b). The precipitation sensitivity to temperature between the future (2060–2099) and historical (1960–1999) periods presented an increasing trend across all precipitation percentiles over the high-latitude regions (>60°). Conversely, a widespread decline in precipitation sensitivity to temperature was witnessed in most precipitation percentiles across the low and middle latitudes (≤60°). Notably, an overall increasing trend in precipitation sensitivity to temperature was detected for extreme precipitation (percentiles >99th) across all latitude gradients (Figure 1c). The standard deviation of precipitation among the models revealed high variability with light and middle precipitation (percentiles <50th), which may be related to the strong effect of circulation changes, as CMIP6 models show little overall improvement for the summer monsoons (Fiedler et al., 2020). In contrast, low variability was observed in heavy and extreme precipitation, suggesting a consistent and robust increase in the projected extreme precipitation among the models (Figure 1d).

3.2. Global Patterns of Precipitation Response to Temperature

To identify where and how strongly climate warming impacts precipitation, we calculated the differences in extreme and mean precipitation between historical and future periods. Subsequently, we estimated the sensitivity of precipitation to global warming by dividing this difference by the change in global mean temperature (ΔGSAT). We found that both extreme and mean precipitation sensitivities exhibited similar spatial patterns. However, the magnitude of the sensitivity of extreme precipitation was much larger than that of the mean precipitation. The extreme precipitation sensitivity revealed a strong increase (>30%/K) in the central region of Africa, the Tibetan Plateau, India, the Arabian Peninsula, and Southeast Asia, whereas regions with a reduction (<−4%/K) in η_{99}

10.1029/2023EF003617

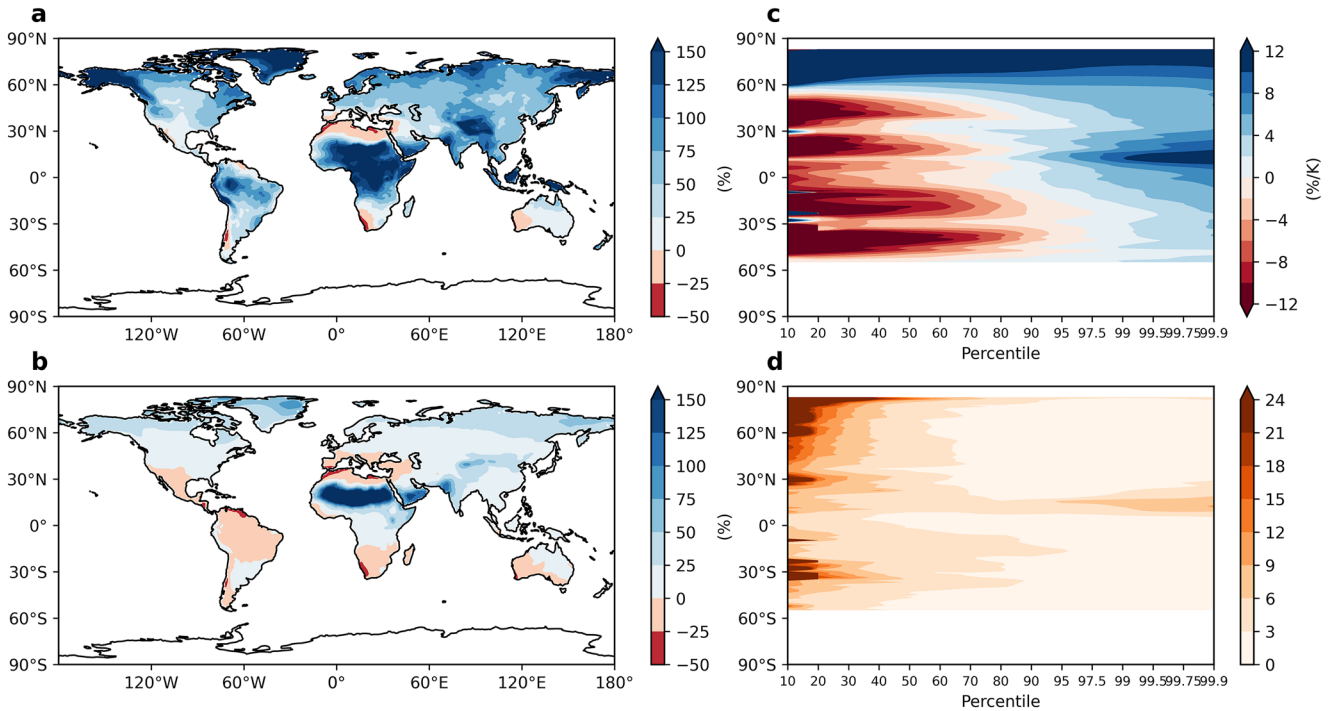

Figure 1. The multi-model ensemble mean (MMEM) precipitation change (%) of extremes (a) and averages (b) from the historical 1960–1999 period to the projected future 2060–2099 period, respectively, from 17 CMIP6 models under the SSP-5.85 scenario. Panel (c) shows the temperature sensitivity of precipitation change between 1960–1999 and 2060–2099 on the latitude and percentile scales over the global land area. Panel (d) is the same as (c) but for the standard deviation of precipitation sensitivity to temperature across models. In Panel (c), the latitudinal-mean precipitation change (%) is divided by ΔGSAT (K).

primarily occurred along the western coastlines of the continental land masses, spanning across Australia, South America, and Africa, in addition to the Mediterranean coastal regions (Figures 2a and 2b). Middle and northern Africa, particularly the Sahara region, showed a large increase in η_{99} and η. These results suggest that a larger η_{99} and η might increase regional precipitation variability; thus, posing a challenge to the sustainability of dry regions ecosystems under future global warming.

On further examination of the frequency distribution of different sensitivities, we showed that the global-mean (area-weighted) sensitivity for extreme precipitation on the land area was three times (19%/K) larger than that for the mean precipitation (6%/K), the latter being close to Clausius–Clapeyron relationship (~7%/K). We futher estimated that the result for the global area was 16.5%/K for η_{99} and 3.5%/K for η (Figure S1 in Supporting Information S1), consistent with prior research. We also discovered very large sensitivities in the East Pacific, which may be associated with the "warmer gets wetter" mechanism over the ocean (Chadwick et al., 2013; Fischer & Knutti, 2015). Additionally, the results indicated a widespread increase in both η_{99} and η across global land areas, with the regions with increased and decreased sensitivities accounting for 94% and 6% for extreme precipitation, whereas those for the mean precipitation were 79% and 21%, respectively (Figures 2c and 2d). We repeated the above analysis at SSP-3.70 scenario simulations and found similar results, with a mean precipitation of 5.5%/K and an extreme for 18%/K, respectively (Figure S2 in Supporting Information S1), highlighting the robustness of these results.

3.3. Asymmetrical η_{99} and η Across Global Dry and Wet Regions

To gain insight into the changes in sensitivity across the dry and wet regions, we classified global land areas into dry and wet regions based on the historical annual extreme and mean precipitation from 1950 to 2014, respectively (Figures 3a and 3b). For dry regions, the sensitivity of extreme precipitation was ~22%/K, whereas that, for mean precipitation was ~11%/K. For wet regions, the sensitivity of extreme precipitation was ~19%/K, whereas that for mean precipitation was ~2%/K. This result suggests that the temperature sensitivities of precipitation in global dry regions are significantly stronger than those in wet regions, with a five-fold higher temperature sensitivity

10.1029/2023EF003617

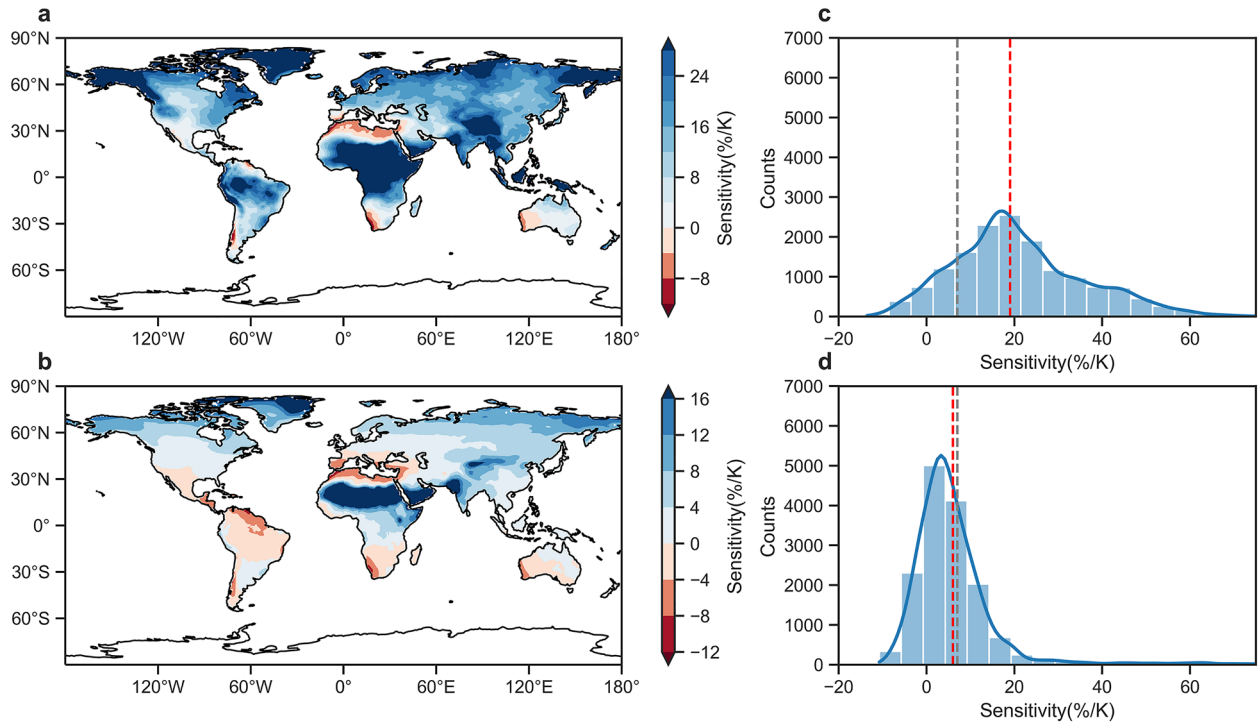

Figure 2. The multi-model ensemble mean (MMEM) temperature sensitivity of the extreme (a) and mean (b) precipitation. The sensitivity is the ratio of the normalized anomaly precipitation (dP, unit: %) to global-mean air temperature change (ΔGSAT, unit: K) from the historical 1960–1999 period to future 2060–2099 period. Panels (c) and (d) present the data distributions in panels (a) and (b), respectively. Colorbars in panels (a) and (b) are different on the positive axis. In panels (c) and (d), the red line is the global-mean (area-weighted) η_{99} (η) values, and the gray line represents the rate of the Clausius–Clapeyron relationship (~7%/K).

for mean precipitation and a minor higher for extreme precipitation. Different models also show a spread in the extreme and mean precipitation sensitivities between dry and wet regions (Figures 3c and 3d), reflecting inter-model variability over different climatic zones (Yazdandoost et al., 2021).

To eliminate the potential influence of dynamic changes in the distribution of dry or wet regions, we calculated sensitivities by constraining regions that remained consistently dry or wet from historical (1950–2014) to future (2036–2100) periods. The analysis revealed consistent results with asymmetrical η (η_{99}) values across global dry and wet regions (Figure S3 in Supporting Information S1). The SSP3-7.0 scenarios also agreed with these findings (Figure S4 in Supporting Information S1). Additionally, we repeated the experiments at a global scale and found a larger η (η_{99}) value in dry regions than in wet regions, similar to the findings from global land regions (Figure S5 in Supporting Information S1). These results suggest that precipitation in dry regions may show a greater sensitivity to temperature under global warming. With the intensification of global warming in dry areas in future, these regions will experience greater variability in precipitation.

3.4. Coupling of η_{99} and η Across Global Wet and Dry Regions

To analyze the potential coupling mechanisms between the mean and extreme precipitation sensitivity across dry and wet regions, we further calculated the correlation coefficient between η_{99} and η across global wet and dry regions (Figure 4). The results indicate that precipitation in dry regions is more sensitive to global warming and there is a higher correlation coefficient between extreme and mean precipitation sensitivities. For instance, the correlation coefficients between η_{99} and η were 0.92 ($p < 0.01$, based on extreme precipitation partition) and 0.93 ($p < 0.01$, based on mean precipitation partition), respectively, for the global dry regions. However, the correlation of these two sensitivities weakened for wet regions, with correlation coefficients of 0.67 ($p < 0.01$) and 0.68 ($p < 0.01$), respectively.

We examined our results for the regions classified by more than five models (Figure S6 in Supporting Information S1) and found similar results with stronger correlations between η_{99} and η in the dry regions (0.92 and

10.1029/2023EF003617

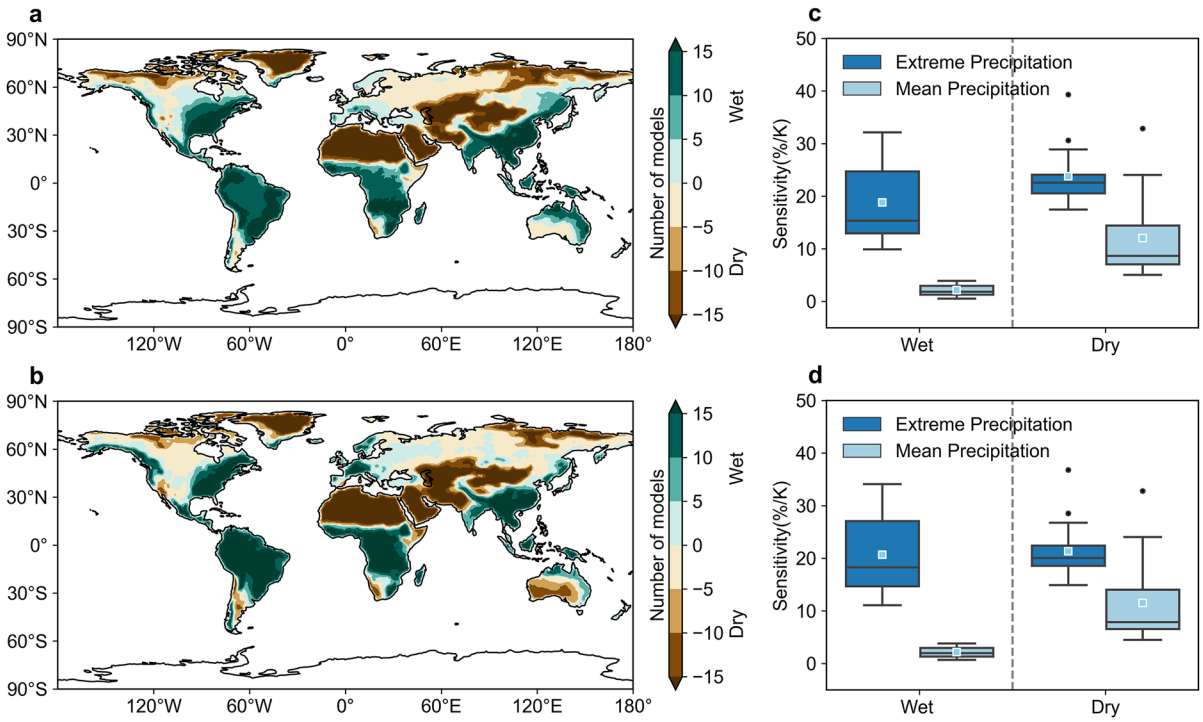

Figure 3. Sensitivity of precipitation to temperature in the wet and dry regions identified by the ensemble of CMIP6 models. Panels (a)and (b) show the spatial pattern of global dry and wet regions classified by the extreme and mean precipitation index from 1950 to 2014, respectively. The extreme (mean) precipitation index contained two percentile-based thresholds of 30% and 70% of the historical annual extreme (mean) precipitation during 1950–2014. Global dry (or wet) regions are those where the precipitation is lower (or higher) than the 30% (70%) threshold. Panels (c) and (d) display the temperature sensitivities of extreme and mean precipitation across models. The solid line in boxplots represents the median sensitivity values of models. The square represents the average values.

0.92) than those in the wet regions (0.81 and 0.84). The SSP3-7.0 scenarios also agreed with these findings (Figure S7 in Supporting Information S1). Additionally, we conducted similar analyses in global regions to ensure the robustness of these findings. The results indicated that η_{99} and η showed a stronger correlation for global dry regions than for wet regions, with values of 0.69 and 0.70 for dry regions and 0.55 and 0.45 for wet regions, respectively (Figure S8 in Supporting Information S1).

4. Discussions and Conclusions

Based on the latest CMIP6 precipitation and temperature projections, we observed that the projected changes in global precipitation are latitude-dependent with an overall increasing trend for extreme precipitation (percentiles ≥99th) across all latitudes. Our results indicate a nearly three-fold increase in the sensitivity of extreme precipitation to global mean surface temperature changes (19%/K) compared with that for mean precipitation (6%/K, reasonably close to the C−C relationship of ∼7%/K). Here, we focused on the response of land precipitation to global warming. Land warming occurs to a greater extent than global warming, which may induce a bit larger sensitivity here (Table S2 and Figure S9 in Supporting Information S1). Nevertheless, these findings suggest the potential for higher flood risk over land regions under changing climatic conditions. We also found greater η and η_{99} across dry regions relative to wet regions worldwide under a warming climate, which is vital for the stability of dryland ecosystems. Since dry regions are a vital component of the carbon cycle globally, an increase in η (η_{99}) in dry regions may alter the variability in precipitation and therefore threaten the dryland ecosystem and global carbon budget. Moreover, poor infrastructure in most dry regions makes them prone to extreme and high-intensity rainfall events (Liu et al., 2023). Urgent adaptation measures are required in dry regions to cope with the projected changes in future hazards driven by global warming. A deeper understanding of the response of precipitation to temperature across different climates will facilitate better planning and management of future extreme events.

We also reported a stronger coupling between extreme and mean precipitation temperature sensitivities in dry regions than in wet regions. An equivalent study was conducted under the SSP3-7.0 scenario, and the results were

10.1029/2023EF003617

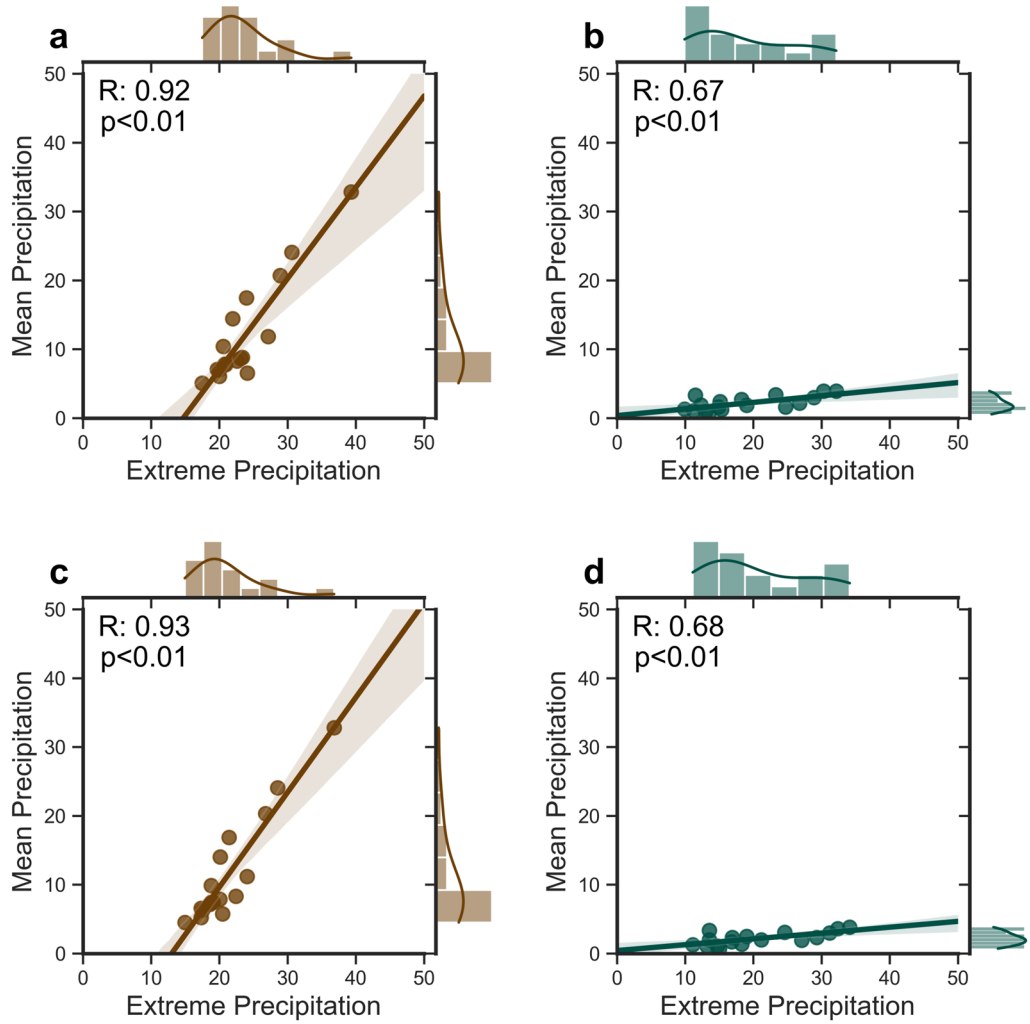

Figure 4. Correlation between the mean and extreme precipitation sensitivity in global dry (in brown color) and wet (in green color) regions. This is demonstrated by scatter plots of mean precipitation changes across the globe against extreme precipitation changes in different CMIP6 models (with each dot representing one model). Panels (a) and (b) were obtained from the extreme precipitation partition, whereas subplots c and d were obtained from the mean precipitation partition.

found to be similar to those of the SSP5-8.5 scenario (Figures S2, S4 and S7 in Supporting Information S1). The stronger η and η_{99} in dry regions may relate to thermodynamic mechanisms (Roderick et al., 2015; Sherwood & Fu, 2014), circulation changes (Chadwick et al., 2013; Chou et al., 2009; Vecchi et al., 2006), and land–atmospheric feedbacks (Berg et al., 2016; Zhou et al., 2019). The lack of surface moisture and evaporative cooling amplifies regional surface warming in dry regions compared with that in humid lands and oceans. We calculated the proportion of extreme precipitation from the total annual precipitation. It was observed that extreme precipitation accounted for 36%–37% of the total annual precipitation for dry regions, while that for wet regions was 19%–21%. These results suggest a tight coupling between extreme and mean precipitation in dry areas relative to that in wet regions (Figure S10 in Supporting Information S1). Therefore, both mean and extreme precipitation are likely to intensify in most global land regions by the end of the 21st century, and the intensification of extreme precipitation in dry regions in particular would inevitably lead to flood risk and adverse impacts on dry ecosystems (Donat et al., 2016; Yao et al., 2021).

We further calculated the correlation coefficient between the η_{99} and η across tropical (<30°) and extratropical (30–60°) land regions, and found significant differences between the two, with a much greater difference in correlation observed in wet regions than in dry regions (Figures S11 and S12 in Supporting Information S1). These findings may be related to the large uncertainties in model simulations of extratropical land regions

(O'Gorman, 2012; Pendergrass et al., 2015; Tabari et al., 2019). The internal variability becomes an important contributor in the model uncertainty, weakening the coupling between η_{99} and η in the extratropical land regions, with correlation coefficients of 0.52 ($p < 0.5$) and 0.44 ($p < 0.1$).

Our study also has several limitations. First, the uncertainty and reliability of climate models vary across regions, which may have influenced our results. For example, extreme and mean precipitation sensitivity results show high standard deviations across models over Africa (Bao et al., 2017; Pendergrass et al., 2015). In this study, we used a multi-model ensemble mean approach to minimize the effects of the strong biases associated with individual models. Second, the different thresholds adopted to define extreme precipitation can affect the temperature sensitivity results (Alexander et al., 2019). Finally, we evaluated the individual CMIP6 models on their native grids and calculated the ensemble mean results after bilinear resampling onto a common $1° \times 1°$ grid (Thackeray et al., 2022). The re-gridding process may have had only a minor effect on the results. Nevertheless, our findings provide a perspective on the response of precipitation to global warming and can be used to plan extreme precipitation events, particularly in dry regions.

Conflict of Interest

The authors declare no conflicts of interest relevant to this study.

Data Availability Statement

We would like to acknowledge the World Climate Research Programme's Working Group on Coupled Modelling. We thank the climate modeling groups for producing and making their model outputs available (Eyring et al., 2016). The data is available at https://esgf-node.llnl.gov/search/cmip6/. Codes are available from: https://doi.org/10.5281/zenodo.7630041.

Acknowledgments
This study was sponsored by the National Natural Science Foundation (Grants: 42171095; 42371123), the Social Science Foundation of Shaanxi Province (Grant: 2020D039), the Fundamental Research Funds for the Central Universities (Grant: GK202201008), and the Open Foundation of the State Key Laboratory of Urban and Regional Ecology of China (Grant: SKLURE2022-2-1).

References

AghaKouchak, A., Chiang, F., Huning, L. S., Love, C. A., Mallakpour, I., Mazdiyasni, O., et al. (2020). Climate extremes and compound hazards in a warming world. *Annual Review of Earth and Planetary Sciences*, *48*(1), 519–548. https://doi.org/10.1146/annurev-earth-071719-055228

Alexander, L. V., Fowler, H. J., Bador, M., Behrangi, A., Donat, M. G., Dunn, R., et al. (2019). On the use of indices to study extreme precipitation on sub-daily and daily timescales. *Environmental Research Letters*, *14*(12), 125008. https://doi.org/10.1088/1748-9326/ab51b6

Allan, R. P., Soden, B. J., John, V. O., Ingram, W., & Good, P. (2010). Current changes in tropical precipitation. *Environmental Research Letters*, *5*(2), 025205. https://doi.org/10.1088/1748-9326/5/2/025205

Allen, M. R., & Ingram, W. J. (2002). Constraints on future changes in climate and the hydrologic cycle. *Nature*, *419*(6903), 224–232. https://doi.org/10.1038/nature01092

Bador, M., & Alexander, L. V. (2022). Future seasonal changes in extreme precipitation scale with changes in the mean. *Earth's Future*, *10*(12), e2022EF002979. https://doi.org/10.1029/2022EF002979

Bao, J., Sherwood, S. C., Alexander, L. V., & Evans, J. P. (2017). Future increases in extreme precipitation exceed observed scaling rates. *Nature Climate Change*, *7*(2), 128–132. https://doi.org/10.1038/nclimate3201

Barbero, R., Fowler, H. J., Lenderink, G., & Blenkinsop, S. (2017). Is the intensification of precipitation extremes with global warming better detected at hourly than daily resolutions? *Geophysical Research Letters*, *44*(2), 974–983. https://doi.org/10.1002/2016GL071917

Berg, A., Findell, K., Lintner, B., Giannini, A., Seneviratne, S. I., van den Hurk, B., et al. (2016). Land–atmosphere feedbacks amplify aridity increase over land under global warming. *Nature Climate Change*, *6*(9), 869–874. https://doi.org/10.1038/nclimate3029

Berg, P., Moseley, C., & Haerter, J. O. (2013). Strong increase in convective precipitation in response to higher temperatures. *Nature Geoscience*, *6*(3), 181–185. https://doi.org/10.1038/ngeo1731

Bourdeau-Goulet, S.-C., & Hassanzadeh, E. (2021). Comparisons between CMIP5 and CMIP6 Models: Simulations of climate indices influencing food security, infrastructure resilience, and human health in Canada. *Earth's Future*, *9*(5), e2021EF001995. https://doi.org/10.1029/2021EF001995

Chadwick, R., Boutle, I., & Martin, G. (2013). Spatial patterns of precipitation change in CMIP5: Why the rich do not get richer in the tropics. *Journal of Climate*, *26*(11), 3803–3822. https://doi.org/10.1175/JCLI-D-12-00543.1

Chen, H., Chen, H., Sun, J., Sun, J., Lin, W., & Xu, H. (2020). Comparison of CMIP6 and CMIP5 models in simulating climate extremes. *Chinese Science Bulletin*, *65*(17), 1415–1418. https://doi.org/10.1016/j.scib.2020.05.015

Chou, C., Neelin, J. D., Chen, C.-A., & Tu, J.-Y. (2009). Evaluating the "Rich-Get-Richer" Mechanism in tropical precipitation change under global warming. *Journal of Climate*, *22*(8), 1982–2005. https://doi.org/10.1175/2008JCLI2471.1

Donat, M. G., Angélil, O., & Ukkola, A. M. (2019). Intensification of precipitation extremes in the world's humid and water-limited regions. *Environmental Research Letters*, *14*(6), 065003. https://doi.org/10.1088/1748-9326/ab1c8e

Donat, M. G., Lowry, A. L., Alexander, L. V., O'Gorman, P. A., & Maher, N. (2016). More extreme precipitation in the world's dry and wet regions. *Nature Climate Change*, *6*(5), 508–513. https://doi.org/10.1038/nclimate2941

Douville, H., Krishnan, R., Renwick, J., Allan, R., Arias, P., Barlow, M., et al. (2021). Water cycle change. In V. Masson-Delmotte, A. Zhai, S. L. Pirani, C. Connors, S. Péan, N. Berger, et al. (Eds.), *Climate change, 2021: The physical science basis. Contribution of working group I to the sixth assessment report of the intergovernmental panel on climate change* (pp. 1055–1210). Cambridge University Press. https://doi.org/10.1017/9781009157896.010

Easterling, D. R., Meehl, G. A., Parmesan, C., Changnon, S. A., Karl, T. R., & Mearns, L. O. (2000). Climate extremes: Observations, modeling, and impacts. *Science*, *289*(5487), 2068–2074. https://doi.org/10.1126/science.289.5487.2068

Eyring, V., Bony, S., Meehl, G. A., Senior, C. A., Stevens, B., Stouffer, R. J., & Taylor, K. E. (2016). Overview of the coupled model intercomparison project phase 6 (CMIP6) experimental design and organization [Dataset]. Geoscientific Model Development, *9*(5), 1937–1958. https://doi.org/10.5194/gmd-9-1937-2016

Fiedler, S., Crueger, T., D'Agostino, R., Peters, K., Becker, T., Leutwyler, D., et al. (2020). Simulated tropical precipitation assessed across three major phases of the coupled model intercomparison project (CMIP). *Monthly Weather Review*, *148*(9), 3653–3680. https://doi.org/10.1175/MWR-D-19-0404.1

Fischer, E. M., & Knutti, R. (2015). Anthropogenic contribution to global occurrence of heavy-precipitation and high-temperature extremes. *Nature Climate Change*, *5*(6), 560–564. https://doi.org/10.1038/nclimate2617

Frei, C., Schöll, R., Fukutome, S., Schmidli, J., & Vidale, P. L. (2006). Future change of precipitation extremes in Europe: Intercomparison of scenarios from regional climate models. *Journal of Geophysical Research*, *111*(D6), D06105. https://doi.org/10.1029/2005JD005965

Greve, P., Orlowsky, B., Mueller, B., Sheffield, J., Reichstein, M., & Seneviratne, S. I. (2014). Global assessment of trends in wetting and drying over land. *Nature Geoscience*, *7*(10), 716–721. https://doi.org/10.1038/NGEO2247

Grose, M. R., Narsey, S., Delage, F. P., Dowdy, A. J., Bador, M., Boschat, G., et al. (2020). Insights from CMIP6 for Australia's future climate. *Earth's Future*, *8*(5), e2019EF001469. https://doi.org/10.1029/2019EF001469

Hausfather, Z., & Peters, G. P. (2020). Emissions—The 'business as usual' story is misleading. *Nature*, *577*(7792), 618–620. https://doi.org/10.1038/d41586-020-00177-3

Held, I. M., & Soden, B. J. (2006). Robust responses of the hydrological cycle to global warming. *Journal of Climate*, *19*(21), 5686–5699. https://doi.org/10.1175/jcli3990.1

John, A., Douville, H., Ribes, A., & Yiou, P. (2022). Quantifying CMIP6 model uncertainties in extreme precipitation projections. *Weather and Climate Extremes*, *36*, 100435. https://doi.org/10.1016/j.wace.2022.100435

Lehmann, J., Coumou, D., & Frieler, K. (2015). Increased record-breaking precipitation events under global warming. *Climatic Change*, *132*(4), 501–515. https://doi.org/10.1007/s10584-015-1434-y

Liu, C., & Allan, R. P. (2013). Observed and simulated precipitation responses in wet and dry regions 1850–2100. *Environmental Research Letters*, *8*(3), 034002. https://doi.org/10.1088/1748-9326/8/3/034002

Liu, L., Ciais, P., Wu, M., Padron, R. S., Friedlingstein, P., Schwaab, J., et al. (2023). Increasingly negative tropical water-interannual CO_2 growth rate coupling. *Nature*, *618*(7966), 755–760. https://doi.org/10.1038/s41586-023-06056-x

Liu, S. C., Fu, C., Shiu, C.-J., Chen, J.-P., & Wu, F. (2009). Temperature dependence of global precipitation extremes. *Geophysical Research Letters*, *36*(17), L17702. https://doi.org/10.1029/2009GL040218

Min, S.-K., Zhang, X., Zwiers, F. W., & Hegerl, G. C. (2011). Human contribution to more-intense precipitation extremes. *Nature*, *470*(7334), 378–381. https://doi.org/10.1038/nature09763

O'Gorman, P. A. (2012). Sensitivity of tropical precipitation extremes to climate change. *Nature Geoscience*, *5*(10), 697–700. https://doi.org/10.1038/ngeo1568

O'Gorman, P. A., & Schneider, T. (2009). The physical basis for increases in precipitation extremes in simulations of 21st-century climate change. *Proceedings of the National Academy of Sciences*, *106*(35), 14773–14777. https://doi.org/10.1073/pnas.0907610106

O'Neill, B. C., Tebaldi, C., van Vuuren, D. P., Eyring, V., Friedlingstein, P., Hurtt, G., et al. (2016). The scenario model intercomparison project (ScenarioMIP) for CMIP6. *Geoscientific Model Development*, *9*(9), 3461–3482. https://doi.org/10.5194/gmd-9-3461-2016

Pendergrass, A. G., & Hartmann, D. L. (2014). The atmospheric energy constraint on global-mean precipitation change. *Journal of Climate*, *27*(2), 757–768. https://doi.org/10.1175/JCLI-D-13-00163.1

Pendergrass, A. G., Lehner, F., Sanderson, B. M., & Xu, Y. (2015). Does extreme precipitation intensity depend on the emissions scenario? Scenario dependence of extreme rain. *Geophysical Research Letters*, *42*(20), 8767–8774. https://doi.org/10.1002/2015GL065854

Prein, A. F., Rasmussen, R. M., Ikeda, K., Liu, C., Clark, M. P., & Holland, G. J. (2017). The future intensification of hourly precipitation extremes. *Nature Climate Change*, *7*(1), 48–52. https://doi.org/10.1038/nclimate3168

Roderick, M. L., Greve, P., & Farquhar, G. D. (2015). On the assessment of aridity with changes in atmospheric CO_2. *Water Resources Research*, *51*(7), 5450–5463. https://doi.org/10.1002/2015WR017031

Screen, J. A., & Simmonds, I. (2014). Amplified mid-latitude planetary waves favour particular regional weather extremes. *Nature Climate Change*, *4*(8), 704–709. https://doi.org/10.1038/nclimate2271

Seneviratne, S. I., Zhang, X., Adnan, M., Badi, W., Dereczynski, C., di Luca, A., et al. (2021). Weather and climate extreme events in a changing climate.

Sherwood, S., & Fu, Q. (2014). A drier future? *Science*, *343*(6172), 737–739. https://doi.org/10.1126/science.1247620

Sun, Q., Miao, C., AghaKouchak, A., Mallakpour, I., Ji, D., & Duan, Q. (2020). Possible increased frequency of ENSO-related dry and wet conditions over some major watersheds in a warming climate. *Bulletin of the American Meteorological Society*, *101*(4), E409–E426. https://doi.org/10.1175/BAMS-D-18-0258.1

Tabari, H., Hosseinzadehtalaei, P., AghaKouchak, A., & Willems, P. (2019). Latitudinal heterogeneity and hotspots of uncertainty in projected extreme precipitation. *Environmental Research Letters*, *14*(12), 124032. https://doi.org/10.1088/1748-9326/ab55fd

Thackeray, C. W., Hall, A., Norris, J., & Chen, D. (2022). Constraining the increased frequency of global precipitation extremes under warming. *Nature Climate Change*, *12*(5), 441–448. https://doi.org/10.1038/s41558-022-01329-1

Trenberth, K. E. (2011). Changes in precipitation with climate change. *Climate Research*, *47*(1), 123–138. https://doi.org/10.3354/cr00953

Trenberth, K. E., Dai, A., Rasmussen, R. M., & Parsons, D. B. (2003). The changing character of precipitation. *Bulletin of the American Meteorological Society*, *84*(9), 1205–1218. https://doi.org/10.1175/BAMS-84-9-1205

Vecchi, G. A., Soden, B. J., Wittenberg, A. T., Held, I. M., Leetmaa, A., & Harrison, M. J. (2006). Weakening of tropical Pacific atmospheric circulation due to anthropogenic forcing. *Nature*, *441*(7089), 73–76. https://doi.org/10.1038/nature04744

Wei, Y., Yu, H., Huang, J., Zhou, T., Zhang, M., & Ren, Y. (2019). Drylands climate response to transient and stabilized 2°C and 1.5°C global warming targets. *Climate Dynamics*, *53*(3), 2375–2389. https://doi.org/10.1007/s00382-019-04860-8

Yao, J., Chen, Y., Chen, J., Zhao, Y., Tuoliewubieke, D., Li, J., et al. (2021). Intensification of extreme precipitation in arid Central Asia. *Journal of Hydrology*, *598*, 125760. https://doi.org/10.1016/j.jhydrol.2020.125760

Yazdandoost, F., Moradian, S., Izadi, A., & Aghakouchak, A. (2021). Evaluation of CMIP6 precipitation simulations across different climatic zones: Uncertainty and model intercomparison. *Atmospheric Research*, *250*, 105369. https://doi.org/10.1016/j.atmosres.2020.105369

Zhang, M., Yu, H., King, A. D., Wei, Y., Huang, J., & Ren, Y. (2020). Greater probability of extreme precipitation under 1.5°C and 2°C warming limits over East-Central Asia. *Climatic Change*, *162*(2), 603–619. https://doi.org/10.1007/s10584-020-02725-2

Zhou, S., Williams, A. P., Berg, A. M., Cook, B. I., Zhang, Y., Hagemann, S., et al. (2019). Land–atmosphere feedbacks exacerbate concurrent soil drought and atmospheric aridity. *Proceedings of the National Academy of Sciences*, *116*(38), 18848–18853. https://doi.org/10.1073/pnas.1904955116